arXiv:1701.06756v1 [cond-mat.mes-hall] 24 Jan 2017

Topological edge state engineering with off-resonant electromagnetic radiation: A route towards topotronics

Mehedi Hasan[1,2], Dmitry Yudin[1], Ivan Iorsh[1,2], Olle Eriksson[3], and Ivan Shelykh[1,4]

[1]ITMO University, Saint Petersburg 197101, Russia
[2]Division of Physics and Applied Physics, Nanyang Technological University 637371, Singapore
[3]Department of Physics and Astronomy, Uppsala University, Box 516, SE-751 20 Uppsala, Sweden
[4]Science Institute, University of Iceland IS-107, Reykjavik, Iceland

We outline here how strong light-matter interaction can be used to induce quantum phase transition between normal and topological phases in two-dimensional topological insulators. We consider the case of a HgTe quantum well, in which band inversion occurs above a critical value of the well thickness, and demonstrate that coupling between electron states and the $E-$field from an off-resonant laser provides a very powerful tool to control topological transitions, even for a thickness of the quantum well that is below the critical value where normally topological edge states occur. We also show that topological phase properties of the edge states, including their group velocity, can be tuned in a controllable way by changing the intensity of the laser field. These findings open up for new experimental means with which to investigate topological insulators. Importantly, all the topological effects discussed here can be realized in a controllable and reversible manner, simply by changing the intensity of the electromagnetic radiation. Technology that relies on these topological states are discussed, hinting towards a possible new field of topotronics.

Topological properties of matter is a subject that recently has received intensified attention, something which draws significant attention of the community of solid state physics and chemistry as well as materials science. The topological classification of time-independent systems was first realized within the paradigm of random matrix theory [1], while later its connection to so called $\mathcal{K}-$theory was discovered [2]. Non-trivial topology of the bulk electronic structure results in the formation of gapless edge modes, which make the surface or interface of the material conducting, while leaving the interior insulating. This is now known as the bulk-boundary correspondence. It turns out that these edge modes are topologically protected, i.e. they are very robust against smooth variations of the material parameters that are relevant for the electronic Hamiltonian. Hence the topological edge states can only be destroyed by closing the bulk gap. Well known examples of topologically protected states are the edge states emerging in quantum Hall phase [3, 4] and topological insulators [5, 6, 7].

Topological protection is commonly portrayed as the key property of topological insulators and the typical example is the so-called $\mathbb{Z}_2$ topological insulator. In the bulk, the topological insulators behave as any other insulators – low or vanishing conductivity. However, when such materials are interfaced with an insulator with a different topological property (e.g., Chern number), conducting states, in which spins of opposite orientation propagate in opposite directions, appear at the boundary between the two materials. This effect is provided by strong spin-orbit coupling which plays a role of an effective spin-dependent magnetic field and thus can be considered as a spin analog of the quantum Hall effect. Following theoretical proposals, topological insulators have been identified experimentally in semiconductors and practically a $\mathbb{Z}_2$ topological insulator is maybe best realized in a HgTe/CdTe quantum well [8], where the existence of edge states has been clearly demonstrated experimentally by measuring quantized resistance [9]. The parameter which conventionally governs the transition to the topological state is the thickness of the HgTe layer: below some critical thickness (approximately 6.1 nm) the system is in the normal

state, while above it, band inversion occurs and a transition to topological state takes place [8]. Clearly, once the structure is grown, the thickness of the layer cannot be changed, and thus transitions between topological and normal states in the same sample cannot be controlled. The main purpose of this paper is to show that this transition can be realized if one uses an additional element of control, namely coupling of the system with an external electromagnetic wave.

In the most general case, the problem of a quantum structure interacting with an external time-dependent field, has no analytic solution and cannot be characterized by well-defined quantum numbers, such as particle energy. Nevertheless, the case of a time-periodic external field can be partially addressed within an equilibrium paradigm, by means of the so-called Floquet expansion [10, 11] which allows the description of the system in terms of quasistationary Floquet states characterized by Floquet quasienergies. The topological classification of periodically driven systems has been proposed in Ref. [12], where it was shown that the dynamical character of a driving field gives rise to a variety of topological phases akin to time-independent ones. Topological properties can be induced even in conventional band insulators, when the system is subjected to a time-periodic perturbation, leading thus to the concept of a Floquet topological insulator [13, 14, 15, 16, 17, 18, 19, 20, 21, 22, 23, 24, 25, 26, 27, 28].

In this paper we demonstrate how the coupling to a time-periodic off-resonant electric field modifies the electronic properties of a $\mathbb{Z}_2$ topological insulator in a non-intuitive but very uesful way. We consider the $\mathbf{k}\cdot\mathbf{p}-$Hamiltonian, appropriate for a HgTe quantum well [7, 29, 30, 31], coupled to a linearly polarized electromagnetic wave that propagates perpendicular to the quantum well interface. By means of Brillouin-Wigner perturbation theory, we obtain an effective time-independent Hamiltonian, in the high-frequency regime. We show that the light-matter coupling in this system leads to a significant renormalization of the parameters of the Hamiltonian that describe the electronic structure. In the most interesting scenario, this renormalization is demonstrated to drive a transition between normal and topological phases, that strongly modifies the properties of the edge states in a controllable and reversible way.

The effective electronic Hamiltonian of a HgTe quantum well sandwiched between CdTe layers can be derived from group-theoretic methods of invariants, or obtained by fitting parameters of the Hamiltonian to results of *ab initio* calculations. Both HgTe and CdTe are characterized by the zinc blende structure with the point-group symmetry of T_d. In the presence of spin-orbit coupling a rotation by 2π changes the sign of the wave function and only three irreducible representations corresponding to two-dimensional Γ_6 and Γ_7 as well as the four-dimensional Γ_8 have to be kept. Therefore, at $\mathbf{k}=0$ each branch of the electronic spectrum transforms according to one of these representations, and in the vicinity of the $\Gamma-$point the $\mathbf{k}\cdot\mathbf{p}-$Hamiltonian of a HgTe quantum well can be written as [7, 29, 30, 31]

$$\mathcal{H}=\begin{pmatrix} \delta_0-(\mathcal{B}+\mathcal{D})\,k^2 & i\mathcal{A}(k_x+ik_y) & 0 & i\gamma \\ -i\mathcal{A}(k_x-ik_y) & -\delta_0+(\mathcal{B}-\mathcal{D})\,k^2 & i\gamma & 0 \\ 0 & -i\gamma & \delta_0-(\mathcal{B}+\mathcal{D})\,k^2 & -i\mathcal{A}(k_x-ik_y) \\ -i\gamma & 0 & i\mathcal{A}(k_x+ik_y) & -\delta_0+(\mathcal{B}-\mathcal{D})\,k^2 \end{pmatrix}. \tag{1}$$

In general, δ_0 corresponds to the gap, while the parameters $\mathcal{A}$, $\mathcal{B}$, and $\mathcal{D}$ describe the band dispersion, and as mentioned above, their numerical values may be obtained from first-principles calculations or from experimental data [7, 32]. The parameter γ is purely determined by the interface of the quantum well. The Hamiltonian in Eq. (1) coincides with that of Bernevig-Hughes-Zhang [7] when the interface asymmetry $\gamma=0$. However, γ was recently shown to have a dramatic impact on the properties of quantum wells, as it drives rather strong level repulsion which drastically modifies the electron states and dispersion [30], and for this reason a non-vanishing value should be considered.

We develop here a theoretical description of a Floquet topological insulator in the zinc blende structure. The γ-parameter, and most of the other parameters in the Hamiltonian (1), are kept finite. The geometry we consider throughout the calculations is schematically depicted in Fig. 1. A linearly polarized electromagnetic wave irradiates the quantum well and is assumed to be uniform in the plane of the well. Furthermore, in the vicinity of the $\Gamma-$point we consider dispersion of electron states by a two-dimensional wave vector $\mathbf{k}=(k_x,k_y)$. The time-dependence $\mathcal{H}(t)=\sum\mathcal{H}_n e^{in\omega t}$ is treated via minimal coupling of electron states to the electromagnetic vector potential: $\mathbf{k}\to\mathbf{k}-e\mathbf{A}(t)$, where $\mathbf{A}(t)=\mathbf{E}_0\cos\omega t/\left(\hbar\omega\right)$. The frequency ω of the external driving field is considered to give a dominant energy scale of the problem, and the field is assumed to be polarized along the y axis, i.e. $\mathbf{E}_0=E_0\mathbf{e}_y$ (the choice of coordinate system is shown in Fig. 1). For sake of simplicity, we assume $\mathcal{D}=0$, which dramatically simplifies the calculations and corresponds to the presence of electron-hole symmetry.

In the high-frequency regime of external pumping, Floquet bands become almost uncoupled, making thus the Hamiltonian block diagonal in Fourier space, so that the Floquet operator can be treated as

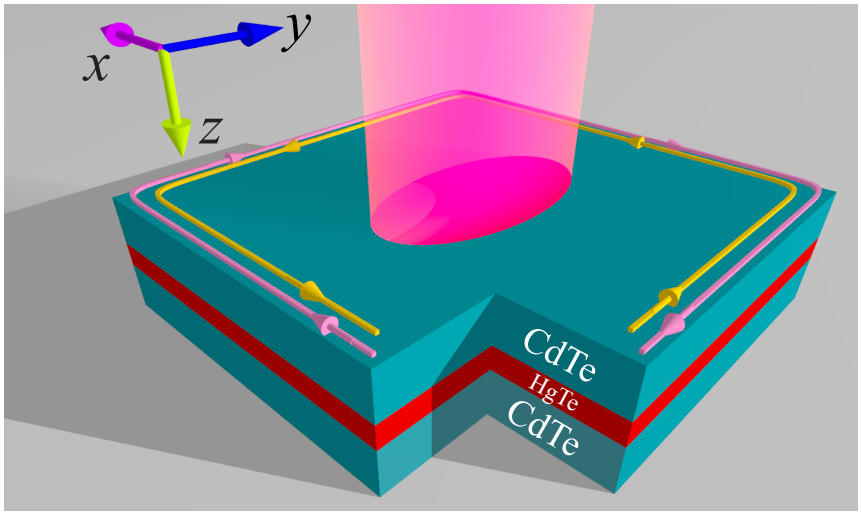

Fig. 1: Geometry of the system under consideration. A HgTe quantum well is sandwiched between CdTe layers and is pumped with highly intense off-resonant electromagnetic field normal to its interface. The coupling between electrons and electromagnetic field modifies the parameters of the Hamiltonian in Eq. (1), which can drive the transition between normal and topological phases, and control the properties of the edge states.

time-independent. The latter permits to fill the bands akin to that of the time-independent systems without any need to estimate the electronic occupancy of Floquet sidebands. The formal derivation of high-frequency effective time-independent Hamiltonian can be performed in a rather intuitive way. In general, for a driven quantum system the effective Hamiltonian makes sense as long as the frequency of a driving field ω is much larger than the bandwidth of the system. The method in question is basically a perturbative expansion with respect to $1/\omega$ and incorporates the effect of weak couplings with neighboring sidebands. A rigorous mathematical procedure may be based on one, out of three alternatives: i) Floquet-Magnus expansion [33, 34, 35, 36] that attempts to write down a stroboscopic evolution operator for a time-independent effective Hamiltonian, ii) van Vleck perturbative series [37, 38] – employing a special ansatz for the time-evolution operator, iii) Brillouin-Wigner perturbation theory – recently proposed for this class of problems [39]. The advantage of utilizing the Brillouin-Wigner perturbation theory is that in contrast to Floquet-Magnus expansion, which explicitly depends on the phase of a driving field, and the van Vleck approach, which generates unlimited number of terms already in lowest orders of perturbative expansion, it is computationally efficient and correctly reproduces well known results of the energy spectrum.

We thus follow the paradigm of high-frequency expansion in the form of Brillouin-Wigner theory [39] to obtain the effective time-independent Hamiltonian in powers of $1/\omega$ that projects the extended Hilbert space to a zero-photon subspace. To zeroth- and first-orders in $1/\omega$ the Hamiltonian remains unchanged, the latter is closely associated with linear polarization of the field for which $\mathcal{H}_{-n} = \mathcal{H}_n$. In principle, higher order terms result in hybridization of nearest Floquet bands. The first non-vanishing correction to the initial Hamiltonian (1), stemming from the terms proportional to $1/\omega^2$, leads to the renormalized Hamiltonian

$$\tilde{\mathcal{H}} = \begin{pmatrix} \tilde{\delta}_0 - \tilde{\mathcal{B}}_x k_x^2 - \tilde{\mathcal{B}}_y k_y^2 & i(\tilde{\mathcal{A}}_x k_x + i\tilde{\mathcal{A}}_y k_y) & 0 & i\tilde{\gamma} \\ -i(\tilde{\mathcal{A}}_x k_x - i\tilde{\mathcal{A}}_y k_y) & -\tilde{\delta}_0 + \tilde{\mathcal{B}}_x k_x^2 + \tilde{\mathcal{B}}_y k_y^2 & i\tilde{\gamma} & 0 \\ 0 & -i\tilde{\gamma} & \tilde{\delta}_0 - \tilde{\mathcal{B}}_x k_x^2 - \tilde{\mathcal{B}}_y k_y^2 & -i(\tilde{\mathcal{A}}_x k_x - i\tilde{\mathcal{A}}_y k_y) \\ -i\tilde{\gamma} & 0 & i(\tilde{\mathcal{A}}_x k_x + i\tilde{\mathcal{A}}_y k_y) & -\tilde{\delta}_0 + \tilde{\mathcal{B}}_x k_x^2 + \tilde{\mathcal{B}}_y k_y^2 \end{pmatrix}. \quad (2)$$

The spectrum of the initial Hamiltonian is given by Eq. 1. Placing the quantum well in a strong electromagnetic field results in a renormalization of δ_0, γ, $\mathcal{A}$, $\mathcal{B}$, and $\mathcal{D}$ (the expressions of $\tilde{\delta}_0$, $\tilde{\gamma}$, $\tilde{\mathcal{A}}_x$, $\tilde{\mathcal{A}}_y$, $\tilde{\mathcal{B}}_x$, and $\tilde{\mathcal{B}}_y$ are listed in the Supplemental Material) in such a way that the final Hamiltonian (Eq. 2) becomes highly anisotropic in $\mathbf{k}-$space. This is in marked contrast to the case of circular polarization, that leads to an increase of the gap only.

It is known from the previous studies that the topologically non-trivial state corresponds to negative

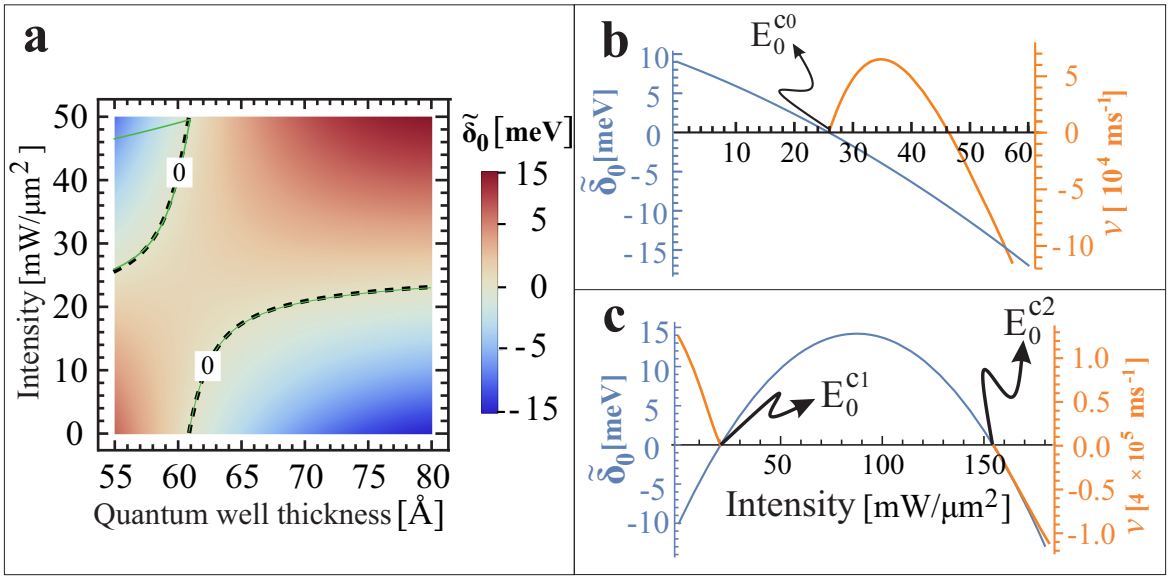

Fig. 2: Light-induced phase transitions under off-resonant pumping with electromagnetic radiation. The phase diagram of the system (a) revealing transitions between topologically trivial and nontrivial states depending on quantum well thickness and intensity of the light. The dashed lines stand for $\tilde{\delta}_0 = 0$ and separate the topological areas, lower right and upper left corners with $\tilde{\delta}_0 < 0$, from the band insulating one (the central region with $\tilde{\delta}_0 > 0$). The green lines in (a) mark the region with zero group velocity of the edge states, $v = 0$. There exists two types of phase transitions as function of intensity of the electromagnetic field: band insulator – to – topological insulator (b) and topological insulator – to – band insulator – to – topological insulator (c). Blue line and left scale show the dependence of the renormalized gap parameter, $\tilde{\delta}_0$, on the pump intensity. Orange line and right scale correspond to the group velocity, v, of the edge states in the topological phase. In the calculations we assume the quantum well thickness is chosen as $d = 5.5$ nm (b), with $\delta_0 = 9$ meV, $\mathcal{A} = 3.87$ eV·Å, $\mathcal{B} = -48$ eV·Å^2, and $d = 7$ nm (c), with $\delta_0 = -10$ meV, $\mathcal{A} = 3.65$ eV·Å, $\mathcal{B} = -68.6$ eV·Å^2.

values of $\mathcal{B}$ and δ_0 of the original Hamiltonian (1). The renormalized value of $\tilde{\delta}_0$ depends on the intensity and the frequency of the driving field as well as the quantum well thickness, and is given by

$$\tilde{\delta}_0 = \delta_0 - \left(\frac{\delta_0\mathcal{A}^2}{2\hbar^2\omega^2} + \frac{\mathcal{B}}{2}\right)\left(\frac{eE_0}{\hbar\omega}\right)^2 + \frac{\left(\delta_0\mathcal{B} + 8\mathcal{A}^2\right)\mathcal{B}}{32\hbar^2\omega^2}\left(\frac{eE_0}{\hbar\omega}\right)^4. \tag{3}$$

From this expression it is clear that by tuning the intensity and frequency of the electromagnetic radiation, one can change the sign of $\tilde{\delta}_0$, something which allows to drive topological transitions in the system solely by optical means. A phase diagram that describes how quantum well thickness and light intensity determine topological and non-topological phases, is presented in Fig. 2a. One can clearly observe that if one starts from a quantum well thickness corresponding to the topologically trivial case, the increase of the intensity of the electromagnetic radiation will lead to a change of the sign of $\tilde{\delta}_0$, causing a transition to the topological phase (upper left corner of Fig. 2a). This is shown in detail in Fig. 2b. At the onset of the topological phase, the group velocity (described in detail below) of the edge states is positive, but a further increase of the intensity of the light leads to the group velocity changing its sign, and the direction of spin currents of the edge are predicted to reverse. On the other hand, if one starts from the topological phase, e.g. in the lower right corner of Fig. 2a, the increase of the light intensity drives the system into a normal phase. However, this case is somewhat more complex, since a further increase of the intensity of the light will bring the system back into a topological phase, as shown in Fig. 2c. As noted in this figure, the spin currents propagate in opposite directions for the two different topological phases (low field and high field phase). Throughout the calculations in Fig. 2, we work with the frequency $\omega = 60$ THz, and other parameters relevant for the calculation are listed in the caption of Fig. 2.

We now proceed with an analysis of the properties of the edge states of the renormalized Hamiltonian (2) analytically. We consider a half infinite plane $x > 0$ occupied by the topological material. Taking

into account the fact that the edge state, in the presence of electron-hole symmetry is a zero-mode, we can write the following equation for the states with $k_y = 0$

$$\tilde{\mathcal{H}}(-i\partial_x, 0)\Psi_{\rm edge}(x) = 0. \tag{4}$$

The solution to (4) results in edge states, which are known to decay exponentially in the bulk, i.e. as $x \to \infty$. These edge states are given by

$$\Psi^{(1)}_{\rm edge} = \mathcal{C}\frac{1}{\sqrt{L_y}}\left(e^{-\lambda_+ x} - e^{-\lambda_- x}\right)\begin{pmatrix} 1 \\ 1 \\ -1 \\ 1 \end{pmatrix}, \quad \Psi^{(2)}_{\rm edge} = \mathcal{C}\frac{1}{\sqrt{L_y}}\left(e^{-\lambda^*_+ x} - e^{-\lambda^*_- x}\right)\begin{pmatrix} 1 \\ 1 \\ 1 \\ -1 \end{pmatrix}, \tag{5}$$

where we have defined normalization factor $\mathcal{C} = \left(\frac{1}{2{\rm Re}\lambda_+} + \frac{1}{2{\rm Re}\lambda_-} - 2{\rm Re}\left(\frac{1}{\lambda_+ + \lambda^*_-}\right)\right)^{-1/2}$, and

$$\lambda_\pm = \frac{\tilde{\mathcal{A}}_x \pm \sqrt{\tilde{\mathcal{A}}_x^2 - 4\tilde{\mathcal{B}}_x\left(\tilde{\delta}_0 + i\tilde{\gamma}\right)}}{2\tilde{\mathcal{B}}_x}. \tag{6}$$

For experimentally relevant parameters of the quantum well two effective length scales can be defined, $\ell_1 = -\tilde{\mathcal{B}}_x/\tilde{\mathcal{A}}_x$ and $\ell_2 = -\tilde{\mathcal{A}}_x/\tilde{\delta}_0$, as well as $k_0 = \tilde{\gamma}/\tilde{\mathcal{A}}_x$, so that $\lambda_1 = -1/\ell_1$ and $\lambda_2 = -1/\ell_2 + ik_0$. If k_y is non-zero yet small, the wave function of the edge states can be approximated by Eqs. (5) multiplied by complex phases $e^{ik_y y}$ corresponding to the propagation along the edges. The high-frequency Hamiltonian (2) can be projected onto these states $\Psi^{(1)}_{\rm edge}e^{ik_y y}$ and $\Psi^{(2)}_{\rm edge}e^{ik_y y}$. Keeping only the linear terms in k_y, we derive an effective Hamiltonian of the edge states in the following form

$$\mathcal{H}_{\rm edge}(k_y) = -\frac{\tilde{\mathcal{A}}_x\tilde{\delta}_0 k_y}{\tilde{\delta}^2 + \tilde{\gamma}^2}\begin{pmatrix} 0 & \tilde{\delta}_0 + i\tilde{\gamma} \\ \tilde{\delta}_0 - i\tilde{\gamma} & 0 \end{pmatrix}. \tag{7}$$

This expression is valid in the regime when $\ell_1 \ll \ell_2, 1/k_0$. The Hamiltonian (7) corresponds to massless Dirac particles with effective group velocity equal to

$$v = -\frac{\tilde{\mathcal{A}}_y\tilde{\delta}_0/\hbar}{\sqrt{\tilde{\delta}^2 + \tilde{\gamma}^2}}. \tag{8}$$

The expression of the group velocity is shown in Figs. 2b–c, and was discussed above. We note here, in addition to the previous discussion, that the possibility to change the group velocity as function of pump intensity opens a unique way to manipulate the direction of the propagation of edge spin currents in the system optically, which could enable several new technologies.

To investigate the validity of the analytical approach described above, we present also results of numerical simulations showing the formation of topological edge states in a finite strip of the material (see the Supplemental Material for details of the numerical calculations). If initially one is in the normal phase (Fig. 3a) without an external field, edge states are absent. An increase of the intensity of the electromagnetic radiation leads to the closing of the gap at the critical value of the field, $E_0 = E_0^{c0}$ (Fig. 3b). A further increase of E_0 is found to cause a transition to the topological phase and edge states appear. The appearance of these edge states becomes clearly visible, as shown in Fig. 3c. On the other hand, if initially the structure is in a topological phase and edge states are present (Fig. 3d), an increase of the field strength to a value $E_0 = E_0^{c1}$ drives the system first into a normal phase, where edge states are absent (Fig. 3e). The normal phase is stable only in the interval $E_0^{c1} < E_0 < E_0^{c2}$, since a further increase causes the topological state to reappear, when the field strength obeys $E_0 > E_0^{c2}$. Note, however that the sign of the group velocity is different in the topological phases appearing in the regimes of low and high pumping field, which physically correspond to the opposite directions of the propagation of edge spin currents in these two cases. Overall our numerical results, shown in Fig. 3, agree with the analytical data shown in Fig. 2.

In this work we have analyzed how the interaction between electrons and an external electromagnetic field modifies strongly the electronic properties of a $\mathbb{Z}_2$ topological insulator. We considered the classical example of CdTe/HgTe/CdTe heterostructure and demonstrated that coupling between electrons in this quasi-two dimensional material and an external electromagnetic field can drive transitions between normal and topological phases. Depending on the thickness of the quantum well we find transitions from

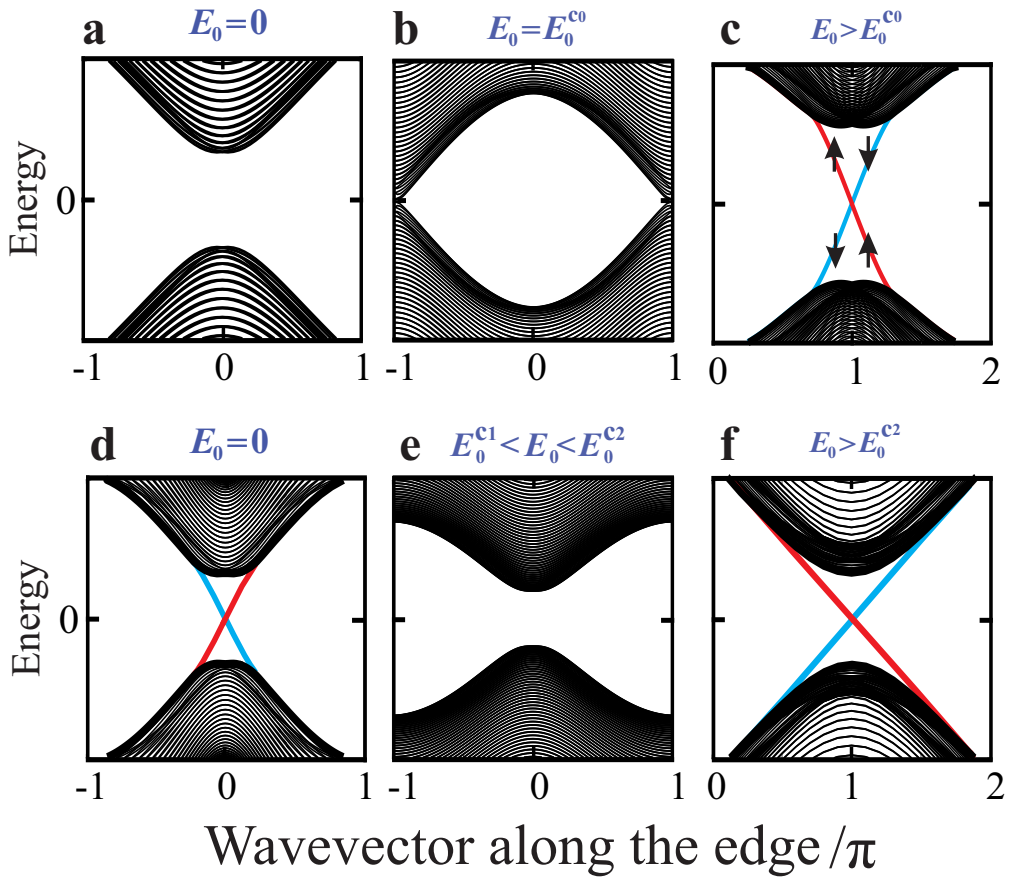

Fig. 3: Band diagram for the finite strip of the CdTe/HgTe/CdTe quantum well. The top panel (a)–(c) describes the evolution of a band insulator – to – topological insulator: in the absence of radiation (a) the system is in a band insulating phase. The increase of the radiation field leads to the quenching of the gap (b) and eventually a transition to the topological phase, when edge states, marked by red (spin-up) and blue (spin-down), show up (c). The bottom panel (d)–(f) corresponds to phase transition from a topological insulator – to – band insulator – to – topological insulator: in the absence of the field (d) edge states are present (red and blue). As the intensity of the radiation goes up the system undergoes a transition to a normal phase, and the edge states disappear (e). Further increase of the intensity of the light causes a transition back to the topological phase (f). Note that directions of spin currents in figures (d) and (f) are opposite, as regimes of low and high pump correspond to the different signs of the group velocity, see Fig. 2c.

a normal state to a topological state, or transitions from a topological state to a normal state back to a topological state, as the intensity of the electromagnetic radiation increases. We have further shown that the light-matter interaction modifies the properties of the edge states in a quite controllable way. In particular, this leads to the creation and control of the edge spin currents.

Our findings open up for new experimental means with which to investigate topological insulators. Importantly, all the topological effects discussed here can be realized in a controllable and reversible manner. This has impact on the development of nanotechnological devices, both concerning prospective spin-optical or electron-optical devices, for instance in the form of transistors, where the electromagnetic field would act as a gate, that turns 'off' or 'on' the conducting edge states shown in Fig. 1. Other technologies that may evolve from our findings relate to the predicted, very controllable group velocity of the edge states. As Fig. 2b shows, by tuning the intensity of the electromagnetic radiation the electrons at the edge can be made to move forwards or backwards, or to be conducting but with an essentially vanishing speed.

We acknowledge the support from the Ministry of Education and Science of the Russian Federation in the framework of Increase Competitiveness Program 5-100, from Singaporean Ministry of Education under AcRF Tier 2 grant MOE2015-T2-1-055 and from Icelandic research fund (Rannis) under projects

141241-053 and 163082-051. D.Y. acknowledges the support from RFBR project 16-32-60040. O.E. acknowledges support from the Swedish Research Council, the KAW foundation (grants 2012.0031 and 2013.0020) and eSSENCE. I.A.S. acknowledges the support from Horizon2020 projects NOTEDEV and CoExAN.

References

[1] Altland, A. & Zirnbauer, M. R. Nonstandard symmetry classes in mesoscopic normal-superconducting hybrid structures. *Phys. Rev. B* **55**, 1142 (1997).

[2] Kitaev, A. Periodic table for topological insulators and superconductors. *AIP Conf. Proc.* **1134**, 22 (2009).

[3] Thouless, D. J., Kohmoto, M., Nightingale, M. P. & den Nijs, M. Quantized Hall Conductance in a Two-Dimensional Periodic Potential. *Phys. Rev. Lett.* **49**, 405 (1982).

[4] Hatsugai, Y. & Kohmoto, M. Energy spectrum and the quantum Hall effect on the square lattice with next-nearest-neighbor hopping. *Phys. Rev. B* **42**, 8282 (1990).

[5] Kane, C. L. & Mele, E. J. Quantum Spin Hall Effect in Graphene. *Phys. Rev. Lett.* **95**, 226801 (2005).

[6] Kane, C. L. & Mele, E. J. $\mathbb{Z}_2$ Topological Order and the Quantum Spin Hall Effect. *Phys. Rev. Lett.* **95**, 146802 (2005).

[7] Bernevig, B. A. & Zhang, S.-C. Quantum Spin Hall Effect. *Phys. Rev. Lett.* **96**, 106802 (2006).

[8] Bernevig, B. A., Hughes, T. L. & Zhang, S.-C. Quantum spin Hall effect and topological phase transition in HgTe quantum wells. *Science* **314**, 1757–1761 (2006).

[9] König, M. *et al.* Quantum spin Hall insulator state in HgTe quantum wells. *Science* **318**, 766–770 (2007).

[10] Grifoni, M. & Hänggi, P. Driven quantum tunneling. *Phys. Rep.* **304**, 229–354 (1998).

[11] Kohler, S., Lehmann, J. & Hänggi, P. Driven quantum transport on the nanoscale. *Phys. Rep.* **406**, 379–443 (2005).

[12] Kitagawa, T., Berg, E., Rudner, M. & Demler, E. Topological characterization of periodically driven quantum systems. *Phys. Rev. B* **82**, 235114 (2010).

[13] Oka, T. & Aoki, H. Photovoltaic Hall effect in graphene. *Phys. Rev. B* **79**, 081406(R) (2009).

[14] Karch, J. *et al.* Dynamic Hall Effect Driven by Circularly Polarized Light in a Graphene Layer. *Phys. Rev. Lett.* **105**, 227402 (2010).

[15] Inoue, J. & Tanaka, A. Photoinduced Transition between Conventional and Topological Insulators in Two-Dimensional Electronic Systems. *Phys. Rev. Lett.* **105**, 017401 (2010).

[16] Lindner, N. H., Refael, G. & Galitski, V. Floquet topological insulator in semiconductor quantum wells. *Nature Phys.* **7**, 490–495 (2011).

[17] Gu, Z., Fertig, H. A., Arovas, D. P. & Auerbach, A. Floquet Spectrum and Transport through an Irradiated Graphene Ribbon. *Phys. Rev. Lett.* **107**, 216601 (2011).

[18] Kitagawa, T., Oka, T., Brataas, A., Fu, L. & Demler, E. Transport properties of nonequilibrium systems under the application of light: Photoinduced quantum Hall insulators without Landau levels. *Phys. Rev. B* **84**, 235108 (2011).

[19] Rechtsman, M. C. *et al.* Photonic Floquet topological insulators. *Nature* **496**, 196 (2013).

[20] Wang, Y. H., Steinberg, H., Jarillo-Herrero, P. & Gedik, N. Observation of Floquet-Bloch States on the Surface of a Topological Insulator. *Science* **342**, 453 (2013).

[21] Katan, Y. T. & Podolsky, D. Modulated Floquet Topological Insulators. *Phys. Rev. Lett.* **110**, 016802 (2013).

[22] Rudner, M. S., Lindner, N. H., Berg, E. & Levin, M. Anomalous Edge States and the Bulk-Edge Correspondence for Periodically Driven Two-Dimensional Systems. *Phys. Rev. X* **3**, 031005 (2013).

[23] Jotzu, G. *et al.* Experimental realization of the topological Haldane model with ultracold fermions. *Nature* **515**, 237 (2014).

[24] Grushin, A. G., Gómez-León, A. & Neupert, T. Floquet Fractional Chern Insulators. *Phys. Rev. Lett.* **112**, 156801(2014).

[25] Kundu, A., Fertig, H. A. & Seradjeh, B. Effective Theory of Floquet Topological Transitions. *Phys. Rev. Lett.* **113**, 236803 (2014).

[26] Dehghani, H., Oka, T. & Mitra, A. Dissipative Floquet topological systems. *Phys. Rev. B* **90**, 195429 (2014).

[27] Sentef, M. A. Theory of Floquet band formation and local pseudospin textures in pump-probe photoemission of graphene. *Nat. Commun.* **6**, 7047 (2015).

[28] Klinovaja, J., Stano, P. & Loss, D. Topological Floquet Phases in Driven Coupled Rashba Nanowires. *Phys. Rev. Lett.* **116**, 176401 (2016).

[29] Gerchikov, L. G. & Subashiev, A. V. Non-monotonic behavior of the energy gap in the film made of a gapless semiconductor. *Sov. Phys. Semicond.* **23**, 1386–1388 (1989).

[30] Tarasenko, S. A. *et al.* Split Dirac cones in HgTe/CdTe quantum wells due to symmetry-enforced level anticrossing at interfaces. *Phys. Rev. B* **91**, 081302(R) (2015).

[31] Durnev, M. V. & Tarasenko, S. A. Magnetic field effects on edge and bulk states in topological insulators based on HgTe/CdHgTe quantum wells with strong natural interface inversion asymmetry. *Phys. Rev. B* **93**, 075434 (2016).

[32] König, M. *et al.* The Quantum Spin Hall Effect: Theory and Experiment. *J. Phys. Soc. Jpn.* **77**, 031007 (2008).

[33] Magnus, W. On the exponential solution of differential equations for a linear operator. *Comm. Pure Appl. Math.* **7**, 649–673 (1954).

[34] Casas, F., Oteo, J. A. & Ros, J. Floquet theory: exponential perturbative treatment. *J. Phys. A: Math. Gen.* **34**, 3379–3388 (2001).

[35] Blanes, S., Casas, F., Oteoc, J. A. & Ros, J. The Magnus expansion and some of its applications. *Phys. Rep.* **470**, 151–238 (2009).

[36] Mananga, E. S. & Charpentier, T. Introduction of the Floquet-Magnus expansion in solid-state nuclear magnetic resonance spectroscopy. *J. Chem. Phys.* **135**, 044109 (2011).

[37] Eckardt, A. & Anisimovas, E. High-frequency approximation for periodically driven quantum systems from a Floquet-space perspective. *New J. Phys.* **17**, 093039 (2015).

[38] Bukov, M., D'Alessio, L. & Polkovnikov, A. Universal high-frequency behavior of periodically driven systems: from dynamical stabilization to Floquet engineering. *Adv. Phys.* **64**, 139–226 (2015).

[39] Mikami, T. *et al.* Brillouin-Wigner theory for high-frequency expansion in periodically driven systems: Application to Floquet topological insulators. *Phys. Rev. B* **93**, 144307 (2016).

Supplemental Material

Derivation of the effective time-independent Hamiltonian

It was mentioned in the main text that in the vicinity of the $\Gamma-$point, specified by a two-dimensional wave vector $\mathbf{k} = (k_x, k_y)$, the Hamiltonian of a HgTe quantum well reads

$$\mathcal{H} = \begin{pmatrix} H_{\mathbf{k}} & i\gamma\sigma_x \\ -i\gamma\sigma_x & H_{\mathbf{k}}^* \end{pmatrix}, \tag{S1}$$

where we have defined $\sigma = (\sigma_0, \boldsymbol{\sigma})$ a set of Pauli matrices equipped with a 2×2 unity matrix. The $2 \times 2-$blocks of the Hamiltonian $H_{\mathbf{k}}$ and $H_{\mathbf{k}}^*$ act on the subspace spanned by the states with total momentum $J_z = 1/2, 3/2$ and $J_z = -1/2, -3/2$ respectively and they are related to each other by time reversal symmetry. An explicit expression for $H_{\mathbf{k}}$ is

$$H_{\mathbf{k}} = -\mathcal{D}k^2\sigma_0 - \mathcal{A}\left(k_y\sigma_x + k_x\sigma_y\right) + \left(\delta_0 - \mathcal{B}k^2\right)\sigma_z. \tag{S2}$$

The time-dependence $\mathcal{H}(t) = \sum \mathcal{H}_n e^{in\omega t}$ is added to the initial Hamiltonian (S1) via the electromagnetic vector potential of the external driving field, $\mathbf{E}(t) = \mathbf{E}_0 \sin\omega t$, with frequency ω (this is assumed to be the dominant energy scale) and with a polarization along the y axis: $\mathbf{E}_0 = E_0\mathbf{e}_y$. Next, we define

$$\mathcal{H}_0 = \mathcal{H} - \frac{\mathcal{B}}{2}\left(\frac{eE_0}{\hbar\omega}\right)^2 \sigma_0 \otimes \sigma_z, \tag{S3}$$

$$\mathcal{H}_1 = \mathcal{H}_{-1} = \left(\frac{eE_0}{\hbar\omega}\right)\left(\mathcal{B}k_y\sigma_0 \otimes \sigma_z + \frac{\mathcal{A}}{2}\sigma_0 \otimes \sigma_x\right), \tag{S4}$$

$$\mathcal{H}_2 = \mathcal{H}_{-2} = \frac{\mathcal{B}}{4}\left(\frac{eE_0}{\hbar\omega}\right)^2 \sigma_0 \otimes \sigma_z, \tag{S5}$$

where $\sigma_0 \otimes \sigma_x$, $\sigma_0 \otimes \sigma_z$ denote the tensor products of a unity matrix with $\sigma_{x,z}$ respectively. For the sake of simplicity, and as mentioned in the main part of the paper, we put $\mathcal{D} = 0$ which corresponds to electron-hole symmetry. The effective renormalized Hamiltonian can be derived within the paradigm of high-frequency expansion in the form of Brillouin-Wigner theory. Up to the terms in $1/\omega^2$ we obtain

$$\tilde{\mathcal{H}} = \mathcal{H} + \frac{1}{(\hbar\omega)^2}\left([\mathcal{H}_1, [\mathcal{H}_1, \mathcal{H}_2]] + 2\mathcal{H}_1\mathcal{H}_0\mathcal{H}_1 + \frac{1}{2}\mathcal{H}_2\mathcal{H}_0\mathcal{H}_2\right). \tag{S6}$$

After straight forward algebra we obtain

$$\tilde{\mathcal{H}} = \begin{pmatrix} \tilde{H}_{\mathbf{k}} & i\left(\tilde{\gamma} + \gamma_y' k_y^2\right)\sigma_x \\ -i\left(\tilde{\gamma} + \gamma_y' k_y^2\right)\sigma_x & \tilde{H}_{\mathbf{k}}^* \end{pmatrix}, \tag{S7}$$

where the 2×2 block

$$\tilde{H}_{\mathbf{k}} = -\tilde{\mathcal{A}}_y k_y\sigma_x - \tilde{\mathcal{A}}_x k_x\sigma_y + \left(\tilde{\delta}_0 - \tilde{\mathcal{B}}_x k_x^2 - \tilde{\mathcal{B}}_y k_y^2\right)\sigma_z. \tag{S8}$$

is formally analogous to $H_{\mathbf{k}}$ with renormalized parameters.

In the formula (S7) we have defined renormalized parameters:

$$\tilde{\gamma} = \gamma\left[1 + \frac{\mathcal{A}^2}{2\hbar^2\omega^2}\left(\frac{eE_0}{\hbar\omega}\right)^2 - \frac{\mathcal{B}^2}{32\hbar^2\omega^2}\left(\frac{eE_0}{\hbar\omega}\right)^4\right]. \tag{S9}$$

It is worthwhile to note that such a procedure generates $\gamma_y' = \frac{2\gamma\mathcal{B}^2}{\hbar^2\omega^2}\left(\frac{eE_0}{\hbar\omega}\right)^2$ which is present in any realistic quantum well structure owing to interface mixing asymmetry. The rest correspond to

$$\tilde{\delta}_0 = \delta_0 - \left(\frac{\delta_0\mathcal{A}^2}{2\hbar^2\omega^2} + \frac{\mathcal{B}}{2}\right)\left(\frac{eE_0}{\hbar\omega}\right)^2 + \frac{\left(\delta_0\mathcal{B} + 8\mathcal{A}^2\right)\mathcal{B}}{32\hbar^2\omega^2}\left(\frac{eE_0}{\hbar\omega}\right)^4, \tag{S10}$$

i.e., a renormalized gap, and

$$\tilde{\mathcal{A}}_x = \mathcal{A}\left[1 + \frac{\mathcal{A}^2 - 4\delta_0\mathcal{B}}{2\hbar^2\omega^2}\left(\frac{eE_0}{\hbar\omega}\right)^2 - \frac{\mathcal{B}^2}{32\hbar^2\omega^2}\left(\frac{eE_0}{\hbar\omega}\right)^4\right], \tag{S11}$$

$$\tilde{\mathcal{A}}_y = \mathcal{A}\left[1 - \frac{\mathcal{A}^2}{2\hbar^2\omega^2}\left(\frac{eE_0}{\hbar\omega}\right)^2 + \frac{15\mathcal{B}^2}{32\hbar^2\omega^2}\left(\frac{eE_0}{\hbar\omega}\right)^4\right], \tag{S12}$$

$$\tilde{\mathcal{B}}_x = \mathcal{B}\left[1 - \frac{\mathcal{A}^2}{2\hbar^2\omega^2}\left(\frac{eE_0}{\hbar\omega}\right)^2 + \frac{\mathcal{B}^2}{32\hbar^2\omega^2}\left(\frac{eE_0}{\hbar\omega}\right)^4\right], \tag{S13}$$

$$\tilde{\mathcal{B}}_y = \mathcal{B}\left[1 - \frac{4\delta_0\mathcal{B} - 3\mathcal{A}^2}{2\hbar^2\omega^2}\left(\frac{eE_0}{\hbar\omega}\right)^2 + \frac{33\mathcal{B}^2}{32\hbar^2\omega^2}\left(\frac{eE_0}{\hbar\omega}\right)^4\right]. \tag{S14}$$

Details of the numerical calculations of edge states

Eq. 2 in the main text corresponds to the bulk Hamiltonian dressed with an off-resonant linearly polarized electromagnetic radiation. To find the edge states for a finite strip in full agreement with [1] the following steps are to be performed:

1. Extension to the whole Brillouin zone according to $k_i \to \sin(k_i a)/a$, and $k_i^2 \to 2(1-\cos(k_i a))/a^2$, where a is the lattice spacing and $i = x, y$.

2. Perform the Fourier transformation along the finite axis (we call it v-axis), so that $\sin(k_v a) \to i\hat{c}^\dagger_{j+1}\hat{c}_j/2$ and $\cos(k_v a) \to \hat{c}^\dagger_{j+1}\hat{c}_j/2$, where k_v is **not** a good quantum number due to to the finite size of the strip and j runs over the lattice sites. For the terms in the Hamiltonian that are free from k_v, i.e. associated with the periodic directions, the substitution results in $g(k_u) \to g(k_u)\,\hat{c}^\dagger_j\hat{c}_j$, where g being an arbitrary function that has no terms relating the wave vector along the direction of finite-strip.

3. The tight-binding equation, at a particular lattice point, can be written as follows,

$$\left[\Gamma^\dagger\ \Psi_{j-1} + \mathcal{F}(\mathbf{k})\,\Psi_j + \Gamma\ \Psi_{j+1}\right] = E\Psi_j, \tag{S15}$$

   where Ψ is the full spinor. Electron and hole bands are designated with subscripts e and h respectively, while up- and down-arrows represent spin direction,

$$\Psi_j = \begin{pmatrix} \psi_{\uparrow,e,j} \\ \psi_{\uparrow,h,j} \\ \psi_{\downarrow,e,j} \\ \psi_{\downarrow,h,j} \end{pmatrix}. \tag{S16}$$

4. Finally, terms from step-2 are equated accordingly, to find the functions $\mathcal{F}(\mathbf{k})$, Γ, and $\Gamma^\dagger$, comparing the terms with step-3. The Hamiltonian for a finite system with four points along the finite dimension reads

$$H_{16\times16} = \begin{pmatrix} \mathcal{F}(\mathbf{k}) & \Gamma & 0 & 0 \\ \Gamma^\dagger & \mathcal{F}(\mathbf{k}) & \Gamma & 0 \\ 0 & \Gamma^\dagger & \mathcal{F}(\mathbf{k}) & \Gamma \\ 0 & 0 & \Gamma^\dagger & \mathcal{F}(\mathbf{k}) \end{pmatrix}, \tag{S17}$$

   Note that Dirichlet boundary condition have been employed in the above matrix.

For all of our calculations, we have used 100 lattice points along the finite axis of the strip and convergence for the number of lattice points has been checked.

References

[1] Shen, Shun-Qing, Topological Insulators: Dirac Equation in Condensed Matters, *Springer* (2012).